Building and Environment 44 (2009) 1362–1370

Contents lists available at ScienceDirect

Building and Environment

journal homepage: www.elsevier.com/locate/buildenv

Estimating the effects of ambient conditions on the performance of UVGI air cleaners

Josephine Lau, William Bahnfleth*, James Freihaut

Indoor Environment Center, Department of Architectural Engineering, The Pennsylvania State University, University Park, PA, USA

ARTICLE INFO

Article history:
Received 2 April 2008
Received in revised form 24 May 2008
Accepted 27 May 2008

Keywords:
Ultraviolet germicidal irradiation
UVGI
UVC lamp performance
Bioaerosol control
Indoor air quality

ABSTRACT

Ultraviolet germicidal irradiation (UVGI) uses UVC radiation produced by low pressure mercury vapor lamps to control biological air contaminants. Ambient air velocity and temperature have a strong effect on lamp output by influencing the lamp surface cold spot temperature. In-duct UVGI systems are particularly susceptible to ambient effects due to the range of velocity and temperature conditions they may experience. An analytical model of the effect of ambient conditions on lamp surface temperature was developed for three common lamp types in cross flow from a convective–radiative energy balance assuming constant surface temperature. For one lamp type, a single tube standard output lamp, UVC output and cold spot temperature data were obtained under typical in-duct operating conditions. Over an ambient temperature range of 10–32.2 °C and an air velocity range of 0–3.25 m/s, measured cold spot temperature varied from 12.7 to 41.9 °C and measured lamp output varied by 68% of maximum. Surface temperatures predicted by the heat transfer model were 6–17 °C higher than corresponding measured cold spot temperatures, but were found to correlate well with cold spot temperature via a two-variable linear regression. When corrected using this relationship, the simple model predicted the cold spot temperature within 1 °C and lamp UVC output within ±5%. To illustrate its practical use, the calibrated lamp model was employed in a simulation of the control of a contaminant in a single-zone ventilation system by an in-duct UVGI device. In this example, failure to account for the impact of ambient condition effects resulted in under-prediction of average space concentration by approximately 20% relative to a constant output system operating at maximum UVC output.

1. Introduction

Ultraviolet radiation is electromagnetic radiation from the portion of the spectrum encompassing wavelengths from 100 to 400 nm. The International Commission on Illumination [1] divides the UV spectrum into three bands; UVA (315–400 nm), UVB (280–315 nm) and UVC (100–280 nm). Ultraviolet germicidal irradiation (UVGI) is the use of radiation mainly from the UVC band to control microorganisms such as viruses and bacteria by damaging their genetic material, thus rendering them incapable of reproducing. For a given level of control, UVGI can significantly reduce ventilation rate and filtration efficiency requirements, which may make it an attractive alternative or complement to these established methods [2].

The two main types of UVC generators are low and medium-pressure mercury vapor lamps [3]. For germicidal applications, low pressure lamps are most effective because they emit most of their radiant energy (~90%) in the germicidal wavelength band at 253.7 nm in the UVC part of the spectrum. Medium-pressure mercury lamps produce a different spectrum with more energy in the UVB range and are used for water disinfection and for treatment of certain skin diseases. Since this study is concerned with UVGI air disinfection, only the characteristics of low pressure lamps are considered.

Lamps are further distinguished from one another by the starting method, which may be hot cathode or cold cathode. The cathodes of hot cathode lamps operate above ambient temperature while those of cold cathode lamps do not. Hot cathode lamps are identical in electrical characteristics to standard preheat design fluorescent lamp which operate on a preheat circuit with a starter. Their electrodes are tungsten filaments coated with an alkaline earth oxide that emits electrons when heated. Each start causes wear on the filament, which eventually fails. Cold cathode lamps have sturdy cylindrical electrodes instead of filaments, and the lamp is started instantly by means of a high voltage rather than by a starter. This type of electrode seldom wears out.

Literature review indicates that the following parameters may affect the life and output of UV lamps:

- *Age*, (total burning time) [3]. Output decreases with accumulated operating hours as the tube gradually loses its ability

* Corresponding author.
E-mail address: wbahnfleth@psu.edu (W. Bahnfleth).

0360-1323/$ – see front matter © 2008 Elsevier Ltd. All rights reserved.
doi:10.1016/j.buildenv.2008.05.015

Nomenclature

A	lamp tube surface area (m^2)
C	concentration (#/m^3)
C_l	function of Pr in Eq. (6) (–)
D	lamp characteristic length (m)
F	outdoor air fraction
G	contaminant source (#/s)
Gr	Grashof number (–)
I	UVC fluence rate ($\mu W/cm^2$)
k	thermal conductivity (W/m K)
k	UV rate constant ($cm^2/\mu W$ s)
Nu	Nusselt number (–)
Pr	Prandtl number (–)
Q	heat transfer rate (W)
Ra	Rayleigh number = $GrPr$ (–)
Re	Reynolds number (–)
S	survival fraction (–)
T_s	temperature(°C)
U	air velocity (m/s)
ε	emissivity (–)
η	filter or UVGI single-pass efficiency (–)
σ	Stefan–Boltzmann constant ($W/m^2 K^4$)

Subscripts

Amb	ambient
Conv	convective
CS	cold spot
d	lamp diameter
d1	axial length parallel to the flow
eff	effective
F	forced convection flow
i	imaginary
l	laminar heat transfer
M	mixed convection flow
N	natural convection flow
Rad	radiative
S	surface
t	turbulent

to transmit the short wavelengths of ultraviolet light. Typical lamps lose roughly 15% of their peak output over time, but some lamps may depreciate 50% or more. The initial rate of capacity loss is quite rapid; therefore manufacturer rating tests are performed after a burn-in period of 100 h. The effect of this initial period for practical purposes is not of great significance because it represents a small fraction of typical lamp life during which output is at or slightly above the rated output.

- *On/off cycling rate* [3]. The higher the cycling rate (frequency of starts), the shorter the life for hot cathode lamps because the tungsten filaments deteriorate with each cycle. The expected life of a typical lamp with relatively infrequent cycling is approximately 1 year of burning time. However, life for different models of lamps may vary by a factor of two or more even at the same cycling rate.
- *Wind chill* (ambient temperature and velocity effects) [4]. Ambient air flow and temperature strongly affect the lamp surface temperature. The coldest spot on the lamp surface controls UV output by changing the vapor pressure of the mercury in the lamp. This phenomenon is commonly called "wind chill" because the lamp surface is generally warmer than the air stream, and in HVAC applications the net effect is cooling. Lamp power, shape, and orientation to the flow also affect the cold spot temperature. Mercury vapor lamp output peaks at approximately 40 °C, as shown in Fig. 1. Wind chill is primarily of concern for in-duct systems because of the range of velocity and temperature to which lamps are subjected in such applications. Peer reviewed literature and publicly available manufacturer's data currently provide little information on wind chill effects and lamp surface temperature distributions and even less on the impact of these effects on UVGI system performance—which is a primary motivation for this research.
- *Humidity* [5]. While humidity does not directly effect lamp output, water molecules in the irradiated air stream will absorb a portion of UV radiation emitted by a lamp in proportion to absolute humidity and path length to the source. Published measurements [5] indicate that the humidity effects on attenuation of radiation by air for typical operating conditions and optical path lengths are negligible. The literature does not discuss the impact of humidity on convective heat transfer and, therefore, on lamp cold spot temperature.

Cycling rate and burning time are cumulative in their effects, while cold spot temperature and humidity have immediate and short term effects. Together, cycling, aging, and ambient conditions can reduce the UV output relative to the rated output of a new lamp by as much as 75%. Consequently, accurate models of lamp behavior are important for sizing and evaluation of UVGI systems. This issue has received little attention in research literature or design guidance.

The objective of this investigation was to develop a model of lamp output as a function of ambient air velocity and temperature and use it to investigate the operating characteristics of in-duct UVGI systems. It was desired that the model should be sufficiently simple and rapid in its execution to be useful for general-purpose simulation of in-duct UVGI devices and system applications. Such a modeling capability is needed in order to more accurately design and predict the performance of UVGI systems.

2. Methodology

A complete, three-dimensional lamp model explicitly accounting for internal details of lamp construction, multi-dimensional conduction through the lamp tube, and external turbulent convection was deemed too cumbersome and computationally intensive for the present purpose. Therefore, a simple analytical modeling approach based on a uniform surface

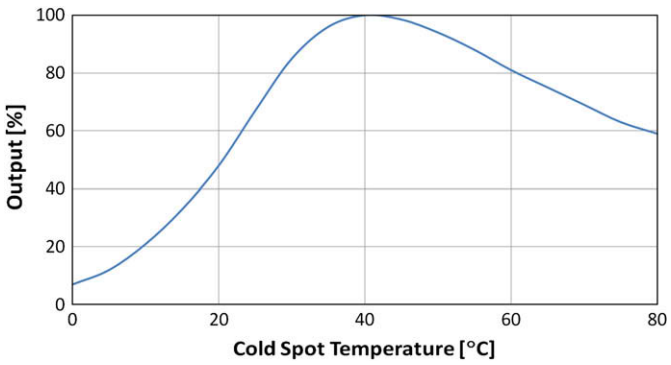

Fig. 1. UV lamp output as a function of lamp surface (cold spot) temperature [3].

temperature assumption was used to qualitatively assess the performance characteristics of several UVC lamp types. For one lamp type, cold spot temperature and output measurements were obtained, compared and correlated with the average surface temperature calculated using the simple analytical model. This correlation was used to correct the output predictions of the analytical model, which was then used in an example of in-duct system simulation intended to indicate the potential discrepancy between the performance of actual in-duct systems and predictions of performance that are not corrected for wind chill effects.

2.1. Lamp type and configurations

Three common UVGI lamp types were studied:

(1) cylindrical hot cathode (Philips TUV 25 W – G25T8),
(2) twin tube hot cathode (Philips TUV PLL 60 W 4P/HO), and
(3) cylindrical cold cathode (Light Sources – 782L10).

Lamp types 1 and 3 are standard output lamps while type 2 is a high output lamp intended to be used in cool conditions. The three lamp types are shown in Fig. 2. Lamp characteristics are summarized in Table 1. Total power input, UVC output, estimated thermal loss, and estimated surface heat flux (thermal loss per unit of lamp tube surface) are shown. The standard output hot cathode lamp (type 1) has both the largest tube diameter and the lowest average surface heat flux of the three while the high output lamp (type 2) has the highest flux. Heat flux and lamp geometry would both be expected to have significant effects on surface temperature for given ambient conditions.

2.2. Analytical model of average lamp surface temperature

The total heat dissipated by a lamp (Q_{Total}) is equal to the input power minus the fraction of input that is emitted as UVC and other non-thermal radiation. The lamp heat balance Eq. (1) includes coupled convective (Q_{Conv}) and radiative (Q_{Rad}) terms.

$$Q_{Total} = Q_{Conv} + Q_{Rad} \tag{1}$$

Total input power was obtained from catalogs. Catalog data and communication with a major manufacturer of UV lamps indicated that approximately 75% of the input power of a typical lamp is dissipated as thermal energy [6]. The sensitivity of this assumption was tested for one of the lamps (type 1) and it was found that between 70% and 80% assumed thermal loss, predicted lamp output varied less than ±3% of the mean value. Based on the analysis of catalog data, the three lamps considered in this study fall roughly within this range.

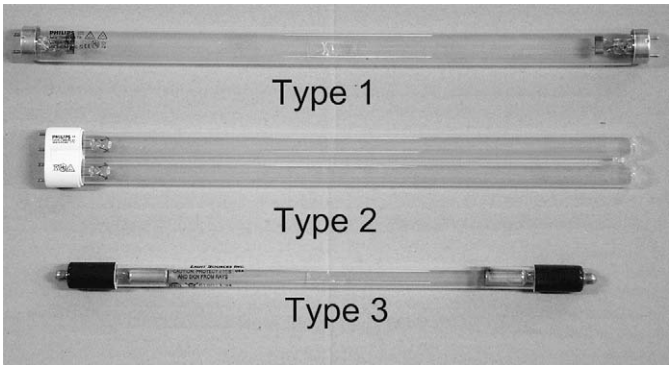

Fig. 2. Modeled lamp types.

Table 1
Lamp characteristics.

Lamp type	1	2	3
Length (mm)	437	385	357
Diameter (mm)	28	18[a]	15
Rated life (hr)	8000	9000	17,500
Input power (W)	25	60	15
UVC output (W)	7	18	2.8
Thermal loss (% of Input)[b]	72	70	81
Surface heat flux[c] (W/m^2)	650	1378	891

[a] Dimension for one tube. Overall width is 38 mm.
[b] Approximated as $100 \times$ (input power − UVC output)/input power.
[c] Thermal loss/surface area.

In terms of the Nusselt number (Nu), the convective heat loss from a lamp is

$$Q_{Conv} = \frac{Nu \cdot k}{D} \cdot A(T_S - T_{Amb}) \tag{2}$$

where k is the thermal conductivity of air, D is the lamp characteristic length (e.g., diameter for a cylinder in cross flow), A is the surface area of the lamp tube, T_S is the average lamp surface temperature, and T_{Amb} is ambient air temperature.

Heat transfer correlations available in the literature for steady-state external convection with constant surface temperature boundary conditions were used to approximate the thermal response of the lamp. The advantage of this approach, as noted previously, is that it is much simpler and more adaptable to system simulation than a full three-dimensional computational fluid dynamics solution with conjugate heat transfer. The limitation of the approach is the known, but unquantified discrepancy found between the surface cold spot temperature and an equivalent uniform average temperature.

Single tube lamps were modeled as infinite cylinders in cross flow. Twin tube lamps were modeled as infinite elliptical cylinders in cross flow. Two cross flow orientations of the twin tube/cylinder lamp were considered: "streamline flow," in which the major axis of the ellipse is parallel to the direction of air flow; and "bluff body flow," in which the major axis is perpendicular to the direction of air flow. In evaluating Eq. (2), D is interpreted as the actual tube diameter for cylindrical lamps and as the stream-wise axial dimension for the ellipse approximating a twin-tube lamp.

The Nusselt numbers for free, mixed, and forced convection regimes were determined by equations valid in different ranges of Reynolds number based on length scale D (forced convection for $Re > 2000$ and mixed convection for lower non-zero values). Eqs. (3) and (4), respectively, give the average Nusselt numbers for natural [7] and forced [8] convection on a cylinder in cross flow (Nu_N and Nu_F, respectively), applicable to lamp types 1 and 3.

$$Nu_N = 0.47(Pr \cdot Gr)^{1/4} \tag{3}$$

$$Nu_F = 0.3 + \frac{0.62 \cdot Re_d^{1/2} \cdot Pr^{1/3}}{\left[1 + \left(\frac{0.4}{Pr}\right)^{2/3}\right]^{1/4}} \left[1 + \left(\frac{Re_d}{282,000}\right)^{5/8}\right]^{4/5} \tag{4}$$

where Pr is the Prandtl number of air (assumed to be 0.71), Re_d is the Reynolds number based on tube diameter, and Gr is the Grashof number.

The forced convection Nusselt number for lamp type 2, which has twin tubes, was approximated by the correlation for an ellipse [9] as shown in Eq. (5):

$$Nu_{d1} = 0.27 \cdot Pr^{0.37} \cdot Re_{d1}^{0.6} \tag{5}$$

where d1 denotes the axial dimension of the ellipse that is parallel to the flow. As described in the referenced source, this correlation was validated with data from ellipses with approximately the same ~2:1 ratio of major and minor axes as the ellipse used to approximate the twin lamp shape in this model.

For natural convection on a horizontal isothermal elliptical cylinder, Eqs. (6)–(8) were used when the major axis of the ellipse was oriented vertically. The estimated Nusselt number (Eq. (8)) is a combination of laminar (Nu_l) and turbulent (Nu_t) values given by Eqs. (6) and (7), respectively.

$$Nu_l = \frac{1.85}{\ln\left(1+\frac{1.85}{0.897\cdot C_l\cdot Ra^{1/4}}\right)} \quad (6)$$

where Ra is the Rayleigh number ($GrPr$), C_l is a function of Pr equal to 0.515 for air.

$$Nu_t = 0.103\cdot Ra^{1/3} \quad (7)$$

$$Nu = \left[(Nu_l)^{10}+(Nu_t)^{10}\right]^{1/10} \quad (8)$$

A correlation for natural convection on an ellipse with a horizontal major axis was not identified. For this case, it was assumed that the natural convection Nusselt number was that of a circular cylinder with a diameter equal to twice the diameter of one of the twin lamp tubes, as this was more closely approximated to the geometry than other alternatives.

The mixed convection Nusselt number (Nu_M) was calculated as shown in Eqs. (9)–(11) [7]. The method used was derived for horizontal cylinders but was used for all. An "imaginary" Reynolds number for natural convection, Re_i, is calculated as shown in Eq. (9), then an effective Reynolds number, Re_{eff}, is calculated as the geometric mean of the imaginary value and Re_d (Eq. (10)) and the Nusselt number is a function of Re_{eff} as shown in Eq. (11).

$$Re_i = \left[\frac{Nu_N}{0.583}\right]^{1/0.471} \quad (9)$$

$$Re_{eff} = \sqrt{Re_i^2+Re_d^2} \quad (10)$$

$$Nu_M = 0.583 Re_{eff}^{0.471} \quad (11)$$

Radiation was modeled using standard methods for gray enclosures (Eq. (12)). The infrared emissivity of the quartz lamp surface was assumed to be 0.93 [10].

$$Q_{Rad} = \varepsilon\cdot A\cdot\sigma\left[(T_S+273)^4+(T_{Amb}+273)^4\right] \quad (12)$$

Where ε is the emissivity of the surface and σ is the Stefan–Boltzmann constant.

2.3. Experimental lamp output and cold spot temperature determination

Lamp UVC output and surface temperature were measured in an ambient condition response test rig (Fig. 3). The rig is a well-insulated flow loop in which average air temperature can be controlled within a range from roughly 7.2–37.7 °C ± 1 °C while average air velocity can be varied from 0.50 to 3.30 m/s ± 0.03 m/s. The temperature and flow rate in the test rig are measured by a thermal dispersion-type flow station (Ebtron Model GTx116-PC) with an accuracy of ±2% of reading. A honeycomb grid flow straightener provides velocity spatially uniform to within ±10% at the test section as measured by a 16-point anemometer traverse.

The lamp cold spot temperature location and magnitude were identified from analysis of thermographic images produced by an infrared (IR) camera (FLIR Systems InfraCAM) with an accuracy of ±2 °C. Infrared thermography was selected for measuring temperature because it is a non-invasive method that provides a complete quantitative picture of the lamp surface temperature distribution. It was found that because temperature sensors bonded to the lamp surface increase thermal resistance locally and intercept radiation that would otherwise pass through the tube they are biased toward giving erroneously high readings. Review of published optical properties of quartz glass [11] indicates that its transmittance in the spectral band sensed by the camera (7.5–13 μm) is essentially zero while its emissivity is in excess of 90% [10]. Therefore, it can be concluded that that the camera will measure the lamp surface temperature, not the temperature of the background visible through the quartz glass.

Lamp type 1 (cylindrical standard output hot cathode lamp, Philips TUV 25 W – G25T8) was tested in cross flow. The lamp was burned in for 100 h prior to the experiment as suggested by manufacturers. Air temperature entering the test section was

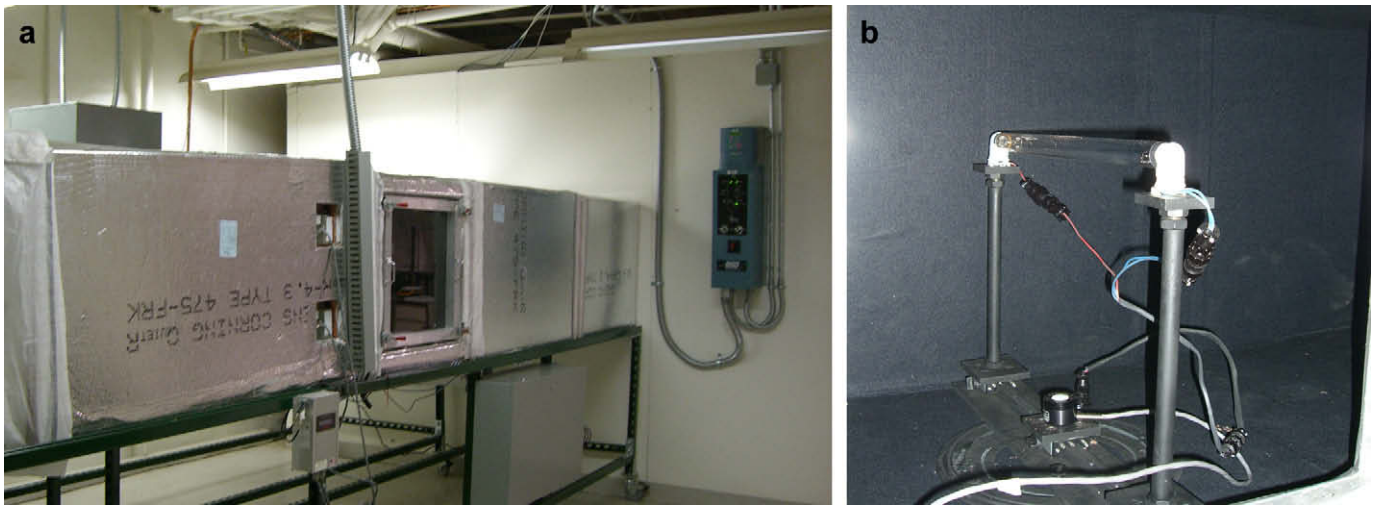

Fig. 3. Ambient condition test rig. (a) exterior view of duct and test section, (b) Close-up of lamp and radiometer in test section.

varied from 10.0 to 32.2 °C and velocity was varied from 0.50–3.25 m/s. UVC output was measured by a research quality radiometer (International Light Technologies, IL 1700 with a silicon photodiode sensor) with an accuracy of ±5.5% of reading located 0.30 m below the center point of the lamp axis (Fig. 3b). Relative UVC output was estimated by comparing the irradiance measured at this location with arbitrary air temperature and flow rate with the same measurement at a condition for which measured cold spot temperature was approximately 40 °C and assumed to be near maximum. Experimental results were then compared with the analytical model developed for average surface temperature.

3. Results

3.1. Constant surface temperature lamp model

Figs. 4–6 show surface temperature predictions obtained with the heat transfer model described above. Each figure presents predicted average surface temperature as a function of air velocity for several values of ambient air temperature. The range of temperature and air velocity shown are representative of the ranges encountered inside typical air-handling units and air distribution ducts.

For each lamp type, as should be expected, surface temperature increases as air velocity decreases (tending to decrease the convective heat transfer coefficient) and as air temperature increases (increasing the heat sink temperature). For a given air temperature, the predicted surface temperature decreases rapidly between zero and ~1 m/s air velocity, as the flow regime moves from pure natural convection toward forced convection. At velocities greater than 2 m/s, the surface temperature is less sensitive to changes in velocity and more sensitive to air temperature.

Lamp type 1 (Fig. 4), which has the largest tube diameter and lowest surface heat flux, operates at the lowest temperate of any of the three lamps. Lamp type 3 (Fig. 5), with smaller tube diameter (therefore, smaller Nusselt number) and higher average heat flux, runs warmer than type 1. The high output lamp type 2 has the highest predicted surface temperatures in bluff body flow orientation (Fig. 6a), but behaves similarly to lamp type 3 in streamline flow (Fig. 6b). It can be seen from Eq. (5) that the Nusselt number for streamline flow will be larger than that for bluff body flow due to the effect of its larger stream-wise length which increases the Reynolds number and, therefore, the Nusselt number. Consequently, the predicted surface temperature should be, and is, lower (Fig. 6b).

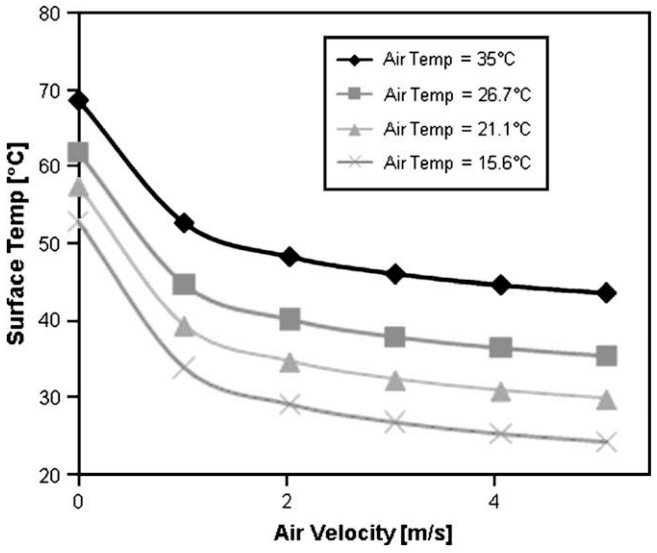

Fig. 4. Predicted Lamp 1 average surface temperature as a function of air velocity and temperature.

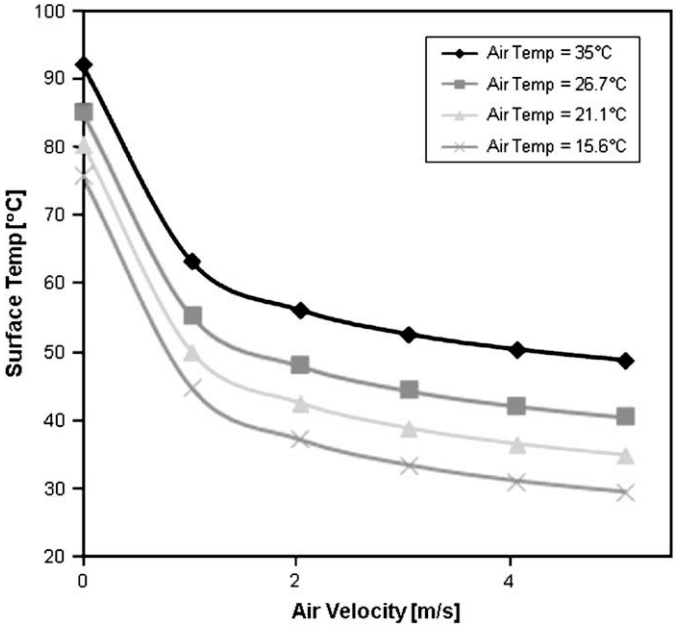

Fig. 5. Predicted Lamp 3 average surface temperature as a function of air velocity and temperature.

The temperature distributions in Figs. 4–6 can be used to estimate lamp UVC output in conjunction with Fig. 1. This has been done by the authors in another paper [12] and is not repeated here. The 40–70 °C range of surface temperatures predicted within the range of ambient conditions considered for each lamp resulted in a predicted wind chill-related UVC output variation of 30–60%. The resulting output distributions are qualitatively very similar to those presented in the limited data made available by lamp manufacturers. The potential significance of output variations of this magnitude for device and system performance provides strong justification for more detailed modeling studies and experimental investigations of lamp performance.

3.2. Air humidity effect on lamp surface temperature

As part of the modeling effort, the sensitivity of predicted average surface temperature results to ambient humidity levels was investigated. Calculations were performed for lamp type 2 in streamline flow orientation with air temperatures varying from 15.6 to 35 °C, air velocity varying from 0 to 5.08 m/s, and relative humidity varying from 0 to 100%. Over this range of conditions, the change in average surface temperature was always less than 0.1 °C, so it is reasonable to assume that this effect, like the UVC absorption effect of humidity, can be neglected in in-duct applications.

3.3. Variable ambient condition lamp surface temperature and output measurements

Measurements of UVC output and cold spot temperature for a type 1 lamp in cross flow were recorded for nine parameter combinations involving three air flow rates (0.51, 1.78 and 3.25 m/s) and three air temperatures (10, 21.1 and 32.2 °C). The cold spot of the lamp, identified by IR thermography, was located at the middle of the lamp axis on the leading edge of the tube. One additional test was performed in still air with an ambient temperature of 21.1 °C to determine a reference value of irradiance for use in calculating relative output, as described previously.

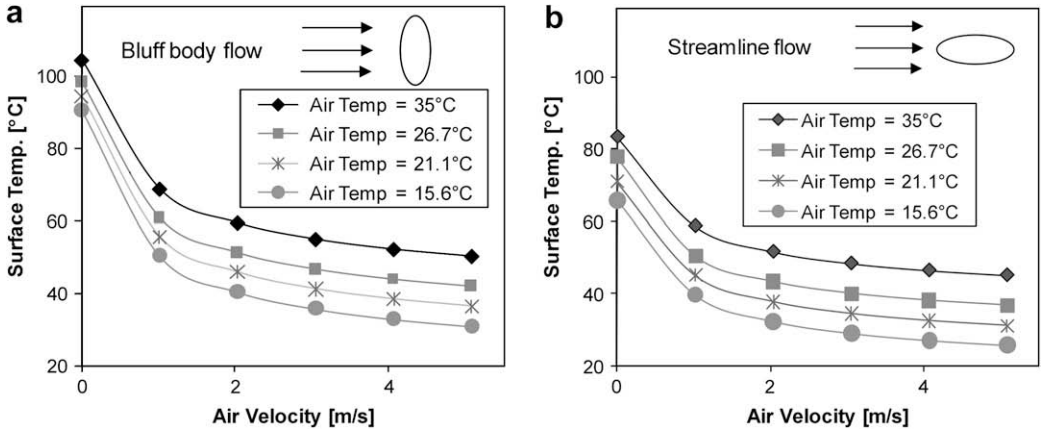

Fig. 6. Predicted Average surface temperature of lamp type 2 for new lamps under different flow conditions (a) bluff body flow and (b) streamline flow.

Results of these 10 tests are summarized in Table 2. Relative UVC output varies from 100% down to a low of 32%. The results agree very well with the manufacturer's data for output vs. cold spot temperature [3], as shown in Fig. 7. A contour plot of UVC vs. air velocity and temperature derived from the measured results is shown in Fig. 8. It shows clearly that output changes more rapidly with air temperature than with air velocity, as was observed in the results of the analytical model presented above.

A regression analysis was performed on the data and a second order function of air temperature and velocity (Eq. (13)) was found to fit the data well (R^2 of 0.96).

$$\text{Output } [\%] = 5.79 + 5.66T_{\text{Amb}} - 20.3U - 0.0701T_{\text{Amb}}^2 + 4.01U^2 \quad (13)$$

For the 10 data points used to generate the regression, the maximum error was 7%, with a mean error of −0.07% and standard deviation of 3.9%. The general good agreement of this model with the data suggests that relatively simple regressions for practical use may be possible, but more data and a higher order model may be needed to reduce the maximum errors to more acceptable levels.

3.4. Comparison of measured cold spot and calculated average surface temperature

In addition to experimental results, Table 2 also includes the calculated average surface temperature for each set of test conditions. The calculated average surface temperature is ~6–17 °C higher than the measured cold spot temperature, with a mean difference of 11.1 °C. Measured cold spot temperature and calculated average surface temperature are shown in a correlation plot in Fig. 9. While lower calculated average surface temperature is correlated with lower cold spot temperature, the nine data pairs also clearly group according to air temperature. Based on this observation, a regression was developed for cold spot temperature (T_{CS}) as a function of calculated average surface temperature computed by the model, and ambient air temperature, all in °C (Eq. (14)).

$$T_{CS} = -2.29 + 0.393T_S + 0.679T_{\text{Amb}} \quad (14)$$

Cold spot temperatures estimated using this model are compared with measured values in Fig. 10. The model and data are clearly in excellent agreement: less than 1 °C difference, which is within the measurement accuracy of the IR camera.

Relative UVC output of lamp type 1 was predicted using a model consisting of (1) prediction of average surface temperature using the analytical model, (2) prediction of cold spot temperature using Eq. (14) and (3) a polynomial approximation of Fig. 1. Agreement was good, as shown in Fig. 11—better than the predictions of the direct second order regression model of the experimental data (Eq. (13)). The largest discrepancies occurred at the highest values of air temperature and velocity. In both Figs. 10 and 11, it is apparent that the impact of air temperature is stronger than that of air velocity, at least within the ranges of values considered, as was observed in the predictions of the simple heat transfer model (Figs. 4–6).

3.5. Example lamp model application

The lamp model developed above, consisting of the simple heat transfer model, Eq. 14, and a polynomial approximation of Fig. 1, can be applied to the analysis of UVGI systems in a variety of ways. One

Table 2
Lamp surface temperatures and lamp output under various conditions.

Air temperature [°C]	Air velocity [m/s]	Cold spot temperature [°C]	Calculated average temperature [°C]	Center irradiance [mW/cm^2]	Relative UVC output [%]
32.2	0.51	41.9	56.6	0.527	99
32.2	1.78	37.8	46.9	0.511	96
32.2	3.25	37.2	43.6	0.505	95
21.1	0.00	39.3	–	0.53	100
21.1	0.51	30.2	46.3	0.44	83
21.1	1.78	26.2	36.1	0.378	71
21.1	3.25	24.6	32.6	0.348	66
10.0	0.51	18.7	36.0	0.238	45
10.0	1.78	14.9	25.2	0.174	33
10.0	3.25	12. 7	21.6	0.168	32

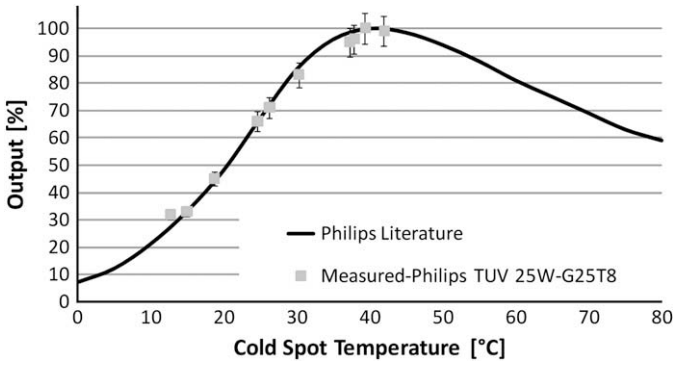

Fig. 7. Measured output vs. cold spot temperature for lamp type 1 compared with manufacturer's data.

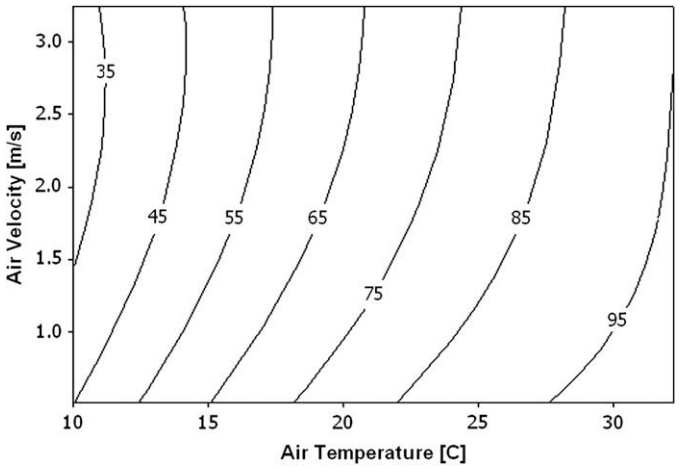

Fig. 8. Lamp UV output vs. air velocity and temperature (contours are % of maximum).

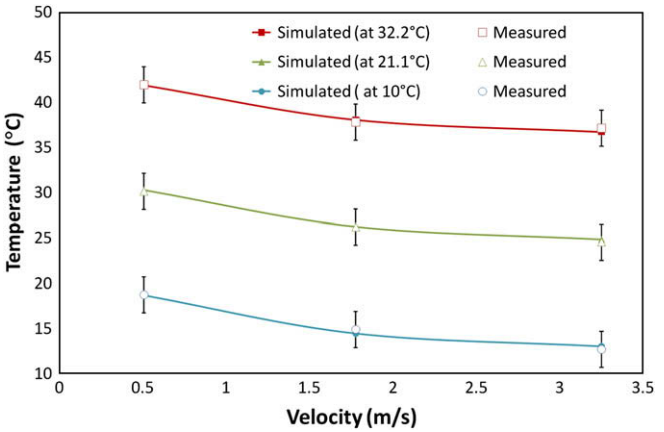

Fig. 10. Comparison between predicted and measured cold spot temperatures at different ambient conditions.

possible application is to use it to adjust lamp output in a detailed analysis of a particular device, in which case it might be imbedded in a CFD model. Another possibility is to use it, and potentially, also a depreciation model, in a simplified system model. The latter application is illustrated through the example of a simple single-zone system with air treated by an in-duct UVGI system. The purpose of this example is to obtain an indication of the magnitude of system-level impact, i.e., the effect of wind chill effects on space concentrations.

Transient simulations of contaminant transport were performed for an internal zone of an office building served by a single-zone VAV system with particulate filtration in the air-handling unit and in-duct UVGI (Fig. 12). The modeled space was treated as a well-mixed zone with no deposition or resuspension of contaminants. The neglect of these affects considerably simplifies the analysis and, because all of the contaminant control modes considered: dilution, particulate filtration, and UVGI are equally affected by these factors, comparisons of their relative performance are not affected. With this simplification, a system the space concentration C (#/m^3) can be determined by solving the following first-order transient differential equation (Eq. (15)).

$$V\frac{dC}{dt} = G + V(1-\eta_{UVGI})\left(1-\eta_{filter}\right)(1-f)C - VC \qquad (15)$$

where V is the volume of the space (m^3), V is supply and return air volume flow rate (m^3/s), f is the ratio of outdoor air to supply air volume flow rate (–), G is the contaminant source strength (#/s), η_{UVGI} is deactivation efficiency of UVGI (%), and η_{filter} is the efficiency of the particulate filter (%).

The building was assumed to be located in Harrisburg, PA (USA). A summer design day with a maximum outdoor dry-bulb temperature of 31 °C was modeled. The conditioned space had a floor area of 557 m^2. Design supply air flow was 2120 m^3/h at a constant supply temperature of 10 °C. Design occupancy was 36 sedentary adults on a daily 9 a.m.–5 p.m. work schedule. The space was ventilated according to ASHRAE Standard 62.1 [14] with a constant 918 m^3/h during occupied periods and 102 m^3/h during unoccupied periods

A generic vegetative bacterium was used as a biological air contaminant. The typical size range of bacteria is approximately 0.2–1.4 μm [13], therefore a representative size of 0.8 μm was selected. A UV susceptibility constant (k) of 0.001 cm^2/μW s, representative of bacteria, was assumed [14]. Current ventilation standards require at least a minimal level of particulate filtration in any system with a wetted coil. The minimum currently permitted by ASHRAE Standard 62.1 [15] is minimum efficiency report value (MERV) 6, as defined by ASHRAE Standard 52.2-1999 [16]. Therefore, a MERV 6 filter with an efficiency of 10% for 0.8 μm particles was assumed to be installed in the air-handling unit.

To a first approximation, the survival fraction S (–) of a population of microorganisms to a UVC fluence rate (spherical irradiance) I (μW/cm^2) for a time interval t (s) can be approximated by a simple exponential function (Eq. (16)).

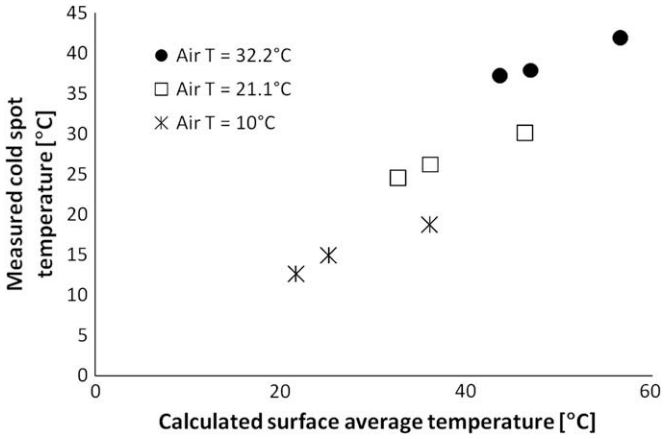

Fig. 9. Measured cold spot temperature vs. modeled average surface temperature for lamp type 1.

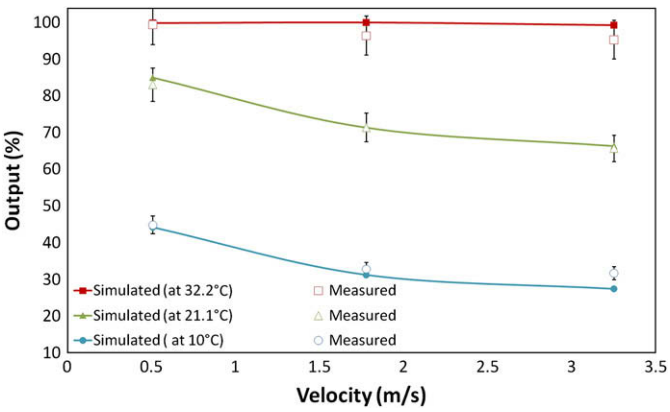

Fig. 11. Comparison between predicted and measured lamp output at different ambient conditions.

$$S = \exp(-kIt) \tag{16}$$

Some microorganisms display more complex dose responses that have been described as "shoulder effect", an initially small response, and "two-stage" response, in which the microorgansim behaves as if the population consists of two fractions, one less resistant and the other more resistant [14]. For the purpose of evaluating the effectiveness of a UVGI system on a particular microorganism, it would be important to model these effects accurately. For the purposes of this example, and given that a generic bacterium was modeled, it was judged that the outcome of the analysis did not depend on such details and the simpler approach was adopted.

Inactivation is the complement of survival, so with the dose response relationship assumed in Eq. (16), the single-pass inactivation efficiency of a UVGI device is

$$\eta_{\mathrm{UVGI}} = 1 - S = 1 - \exp(-kIt) \tag{17}$$

The UVGI model was a "black box" with an assumed single-pass efficiency for the generic bacterium of 99% at system design air flow rate and rated lamp UVC output. The design value of UVC dose (*It* in Eq. (17)) corresponding to 99% inactivation with the assumed microbial *k* value is 4605 μJ/cm^2. Lamps were assumed to have the ambient condition response of lamp type 1 for which the model described above was developed. The velocity through the device at design volume flow rate was assumed to be 4.23 m/s, typical of average velocities in supply air ducts. With these assumptions, the performance of the device could be scaled to different air flows and air temperatures using Eq. (18) with "UVC Output" calculated using the lamp model.

$$It(T_{\mathrm{amb}}, U) = \left[It_{\mathrm{design}}\right] \left(\frac{\text{UVC Output}(T_{\mathrm{amb}}, U)}{\text{UVC Output}_{\mathrm{design}}}\right) \left(\frac{U_{\mathrm{design}}}{U}\right) \tag{18}$$

Four cases were simulated.

- Case 1: UVGI without wind chill correction, MERV 6 filtration, and dilution ventilation.
- Case 2: UVGI with wind chill correction, MERV 6 filtration, and dilution ventilation.
- Case 3: dilution ventilation only.
- Case 4: MERV 6 filtration and dilution ventilation.

Hourly values of occupied space concentration are shown in Fig. 13. Occupied hour (9 a.m.–5 p.m.) average concentration and, where applicable, lamp output results are shown in Table 3. Ventilation alone (Case 3) has the least effect on average space concentration, followed by ventilation + MERV 6 filtration (Case 4) and ventilation + MERV 6 filtration + variable output UVGI (Case 2).

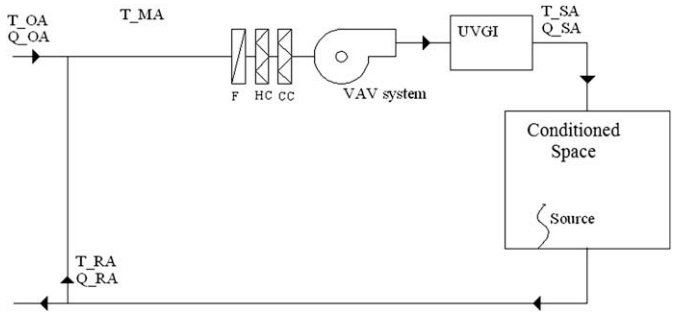

Fig. 12. Schematic diagram of modeled system showing the UVGI device at mix-air branch.

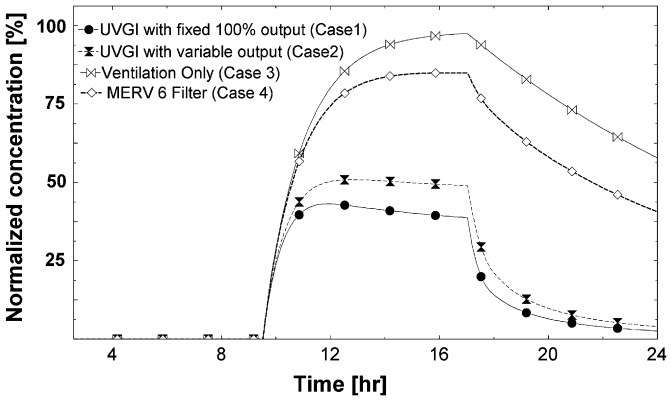

Fig. 13. Normalized conditioned space concentrations for example application.

Case 1 results show that the assumption of constant lamp output in this instance is a poor one that results in significant over-prediction of the effectiveness of UVGI. Average dimensionless space concentration is under-predicted by roughly 20% when no correction is made for wind chill. The substantial incremental impact of UVGI can be observed by comparing concentration results for Case 4 with those for Cases 1 and 2.

Fig. 14 shows supply air velocity (a function of cooling load) and the resulting output of the variable output UVGI model (Case 2) over the course of the simulated day. The relatively high air velocity during the middle of the day combined with the relatively low cooling supply temperature result in a predicted device output, relative to peak capacity, of only 26%. Capacity is higher during the evening and early morning because lower cooling loads during these periods result in lower air velocity across the lamps.

4. Discussion

Manufacturers of UVC lamps have published limited, generic data on the effects of air velocity and temperature on lamp output, but detailed data on specific lamps is not easily accessible. The results of this investigation demonstrate that such wind chill effects may be quite significant for ranges of conditions encountered in induct UVGI applications—nearly 70% variation over the range of conditions considered. This may be of considerable importance in the design of UVGI systems depending upon how they are operated and how critical it is that they provide a consistently high level of performance.

Equipment and procedures for measuring lamp ambient response have been developed and demonstrated. Infrared thermography was found to be applicable to this task and to provide very detailed and useful information. It was shown that the lamp ambient response data can be accurately modeled by simple regressions for direct use in simulation. Further, a simple model of lamp heat transfer based on a uniform surface temperature assumption was shown to correlate well with measured cold spot temperature, which suggests the possibility of a useful semi-empirical lamp model calibrated with limited experimental data.

Table 3
Average concentration and lamp output during occupied hours (9 a.m.–5 p.m.).

Case 1 Constant Output UVGI, Ventilation, MERV 6		Case 2 Variable Output UVGI, Ventilation, MERV 6		Case 3 Ventilation Only	Case 4 MERV 6, Ventilation
Average concentration [%]	Average lamp output [%]	Average concentration [%]	Average lamp output [%]	Average concentration [%]	Average concentration [%]
37.3	100	44.5	26.1	84.0	73.0

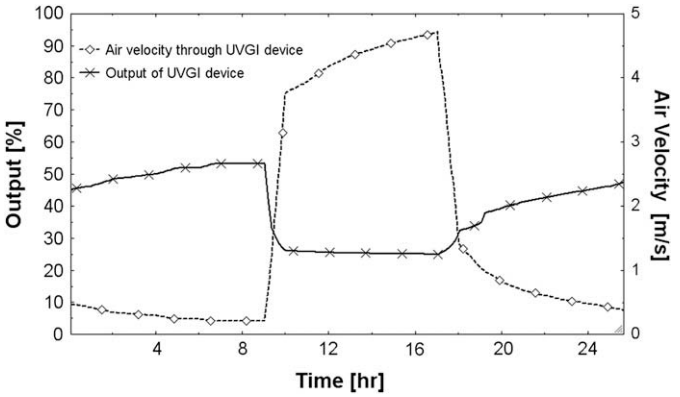

Fig. 14. Supply air flow rate and UVGI device output for example application Case 2.

The example of application of the lamp model described above illustrates the potential magnitude of error that may result from failure to account for ambient effects in the sizing of a UVGI system. In other applications, and with compensated lamps, much better performance could be achieved. However, the potential for very significant underestimates of capacity is demonstrated.

The main limitations of the present work are the simplicity of the thermal modeling of the lamp, restriction of measurements to a single lamp type and orientation on the component level, and the consideration of only one simplified scenario on the system modeling level. There is a need to evaluate other lamp types, especially "compensated" lamps that operate at generally higher temperatures, which have been observed to depreciate to a much greater extent than many standard output lamps. Broader modeling studies combined with economic analysis will help to establish the cost benefit of UVGI more clearly.

The heat transfer modeling method used in this study was simple and exploratory. The observed difference between average lamp surface temperature and cold spot temperature is sufficiently large to make its use without calibration unsatisfactory. However, it proved to work well when corrected using a relatively small number of straightforward experimental measurements. This approach has proved very useful for modeling other complex pieces of HVAC equipment such as chillers. It may, with some improvements, be similarly valuable for modeling UVGI devices.

5. Conclusions

Based on the reported work, the following conclusions can be drawn:

- UVC lamp output variation over the range of conditions encountered in in-duct UVGI applications due to convective "wind chill" effects is significant.
- IR thermography is a useful tool for studying the complex surface temperature distributions of lamps operating in moving airstreams, making location and measurement of the surface cold spot temperature relatively simple.
- There is a significant non-uniformity of surface temperature on a UVC lamp in typical in-duct operating conditions.
- For the practical purpose of modeling wind chill effects, a simple modeling approach calibrated with lamp data may suffice.
- For in-duct applications, ambient air humidity has an effect on lamp output that is negligible for practical purposes.

Use of the measurement and modeling techniques demonstrated in this study may improve the reliability and performance of systems through better design. Better understanding of lamp surface temperature distributions using the experimental methods utilized in this study or through more sophisticated lamp modeling that was beyond the scope of this study may lead to improvements in lamp design that achieve better performance than can be expected from many products currently in use.

Acknowledgement

This work was supported in part by National Center for Energy Management and Building Technologies Task 05-02 and a Graduate Grant-in-Aid from the American Society of Heating, Refrigerating, and Air-Conditioning Engineers. The assistance of Mr. Paul Kremer, research associate, in obtaining the data reported in this paper is gratefully acknowledged.

References

[1] CIE. International lighting vocabulary. Technical Report 17.2–1987. 4th ed. International Electrotechnical Commission/International Commission on Illumination; 1987.
[2] First MW, Nardell EA, Chaisson W, Riley R. Guidelines for the application of upper-room ultraviolet germicidal irradiation for preventing transmission of airborne contagion—part II: design and operation guidance. ASHRAE Transactions 1999;105(1):877–87.
[3] Philips. UV purification – application information. Philips; 2005.
[4] CIE. Ultraviolet air disinfection. Technical Report 155:2003. International Commission on Illumination; 2003.
[5] ARTI. Defining the effectiveness of UV lamps installed in circulating air ductwork; 2002.
[6] Philips. Personal communication with J. Boch. 2007.
[7] Morgan VT. The overall convective heat transfer from smooth circular cylinders. Advances in Heat Transfer 1975;11:199–264.
[8] Churchill SW, Bernstein M. A correlating equation for forced convection from gases and liquids to a circular cylinder in crossflow. Journal of Heat Transfer 1977;99:300–6.
[9] Zhukauskas A, Ziugzda J. Heat transfer of a cylinder in crossflow. New York, NY: Hemisphere Publishing Co.; 1985.
[10] Omega. Emissivity of common materials, http://www.omega.com/literature/transactions/volume1/emissivityb.html; 2005. Available from: [accessed 29.03.08].
[11] Saint-Gobain_Quartz. Properties data sheet of transparent fused Quartz. 2003.
[12] Lau J, Bahnfleth W, Freihaut J. Estimating the effects of ambient conditions and aging on the performance of UVGI air cleaners. In: Proceedings of sixth indoor air quality. Sendai, Japan: Ventilation & Energy Conservation in Buildings; 2007. p. 563–70.
[13] Kowalski WJ. Design and optimization of UVGI air disinfection systems. The Pennsylvania State University; 2001.
[14] Kowalski WJ, Bahnfleth WP, Witham DL, Severin BF, Whittam TS. Mathematical modeling of ultraviolet germicidal irradiation for air disinfection. Quantitative Microbiology 2000;2:249–70.
[15] ASHRAE. ASHRAE Standard 62.1-2007: ventilation for acceptable indoor air quality. Atlanta: ASHRAE; 2007.
[16] ASHRAE. ANSI/ASHRAE standard 52.2: method of testing general ventilation air-cleaning devices for removal efficiency by particle size. Atlanta, GA: American Society of Heating, Refrigerating and Air-Conditioning, Engineers, Inc.; 1999.